Available online at www.sciencedirect.com
SCIENCE DIRECT®
Polymer 44 (2003) 5779–5784
polymer
www.elsevier.com/locate/polymer

Physical aging for an epoxy network diglycidyl ether of bisphenol A/*m*-xylylenediamine

F. Fraga[a,*], C. Castro-Díaz[a], E. Rodríguez-Núñez[a], J.M. Martínez-Ageitos[b]

[a]*Departamento de Física Aplicada, Facultad de Ciencias, Avda Alfonso X El Sabio s/n Universidad de Santiago de Compostela, 27002 Lugo, Spain*
[b]*Departamento de Ingeniería Química, Facultad de Ciencias, Universidad de Santiago de Compostela, 27002 Lugo, Spain*

Received 6 March 2003; received in revised form 23 June 2003; accepted 30 June 2003

Abstract

The physical aging of the epoxy network consisting of a diglycidyl ether of bisphenol A (BADGE n = 0) and *m*-xylylenediamine (*m*-XDA) were studied by differential scanning calorimetry. The following aging temperatures have been used in this work: 60, 70, 80, 90, 100 and 110 °C. The glass transition temperature and the variation of the specific heat capacities have been calculated using the method based on the intersection of both enthalpy–temperature lines for glassy and liquid states. The endothermic aging peak, relaxation enthalpy and fictive temperature were also calculated for each aging temperature and aging time.
© 2003 Elsevier Ltd. All rights reserved.

Keywords: Epoxy-amine reactions; Physical aging; Relaxation enthalpy

1. Introduction

Thermoset polymers generally show an behavior between an elastic solid and a viscous liquid. For this reason these materials are known as viscoelastic and their behavior are determined by a combination of Hooke and Newton laws [1].

Curing reactions of thermoset polymers originate a three-dimensional network after chemical reaction of the epoxy resin and the chosen hardener. During the cure process of a thermoset the glass transition temperature (T_g) of the material increases as a consequence of the increase in the crosslinking density [2]. The transformation from a viscous liquid to an elastic gel is sudden and irreversible and marks the first appearance of the infinite network; it is called the gel point. Gelation is characteristic of thermosets and it occurs at a well-definite and calculable stage in the course of the reaction corresponding to specific values of conversion degree. Other phenomenon that may take place at any stage during cure is vitrification. This transformation from a viscous liquid or elastic gel to a glass begins to occur as the glass transition temperature of the system becomes coincidental with the cure temperature. If this last transition happen during an isothermal curing of epoxy resins at curing temperatures below glass transition temperature could appear an endothermic physical aging peak in the proximity of T_g.

In the last years several articles have been reported above the physical aging in epoxy resins [3–11]. The structural changes produced by physical aging depends of the time and temperature of annealing and show that the behaviour of a thermoset at temperatures below the glass transition are normally the result of slow relaxation of the glass from its initial non-equilibrium state towards its final thermodynamic equilibrium state [12]. These changes can affect its lifetime and therefore in its applications in the industry. A good trace of the structural changes on annealing are the extension of the relaxation enthalpy (Δh) between the original and the annealed glass, and the fictive temperature, hypothetical temperature at which the structure of glass would be in equilibrium.

The epoxy system diglycidyl ether of bisphenol A (BADGE $n = 0$)/*m*-xylylenediamine (*m*-XDA) studied in this work is a very good one to be used both in the building and automobile trades. Therefore we have studied the physical aging for this epoxy network using to calorimetric measurements. Differential Scanning calorimetry was used to calculate the glass transition temperature, specific heat

* Corresponding author. Tel.: +34-982285900; fax: +34-982285872.
E-mail address: franfrag@lugo.usc.es (F. Fraga).

0032-3861/$ - see front matter © 2003 Elsevier Ltd. All rights reserved.
doi:10.1016/S0032-3861(03)00624-4

capacities, endothermic peak temperature, relaxation enthalpy and fictive temperature.

2. Experimental

2.1. Materials

The epoxy resin was a commercial diglycidyl ether of bisphenol A (BADGE $n = 0$) (Resin 332, Sigma Chemical Co. San Louis, USA) with an equivalent molecular weight of 173.6 g/equiv., as determined by wet analysis [13,14]. The curing agent was *m*-xylylenediamine (*m*-XDA, Aldrich Chemical Co., Milwaukee, WI, USA) with an equivalent molecular weight of 31.2 g/equiv.

2.2. Sample preparation

Epoxy resin and curing agent were carefully and homogeneously mixed, at stoichiometric ratio, under a nitrogen atmosphere. The mixture is introduced in a cylindrical frame of 6 mm diameter, previously waxed to avoid adherence. After 24 h at room temperature, the frames are placed for 2 h in an oven at 120 °C. Finally, the samples were cut into 250 μm thickness discs weighing approximately 10 mg.

2.3. Techniques

A differential scanning calorimeter Q100 of TA Instruments was used to obtain all the experimental data reported in this work. The calorimeter requires three calibrations: T_{zero} calibration, cell constant calibration and temperature calibration. The T_{zero} calibration request two experiments: the first one is done without samples; the second one is performed with sapphire disks (without pans) on both the sample and reference position. Both experiments use the same method beginning with equilibration at an initial temperature, holding isothermal for 5 min, heating at constant rate to a final temperature and holding isothermal for 5 min. The range of temperatures necessary for this calibration is between −90 and 400 °C.

The enthalpy constant calibration is based on a run in which one standard metal (indium) is heated through their melting transition. The calculated heat of fusion (28.01 J/g) is compared to the theoretical value (28.39 J/g). The cell constant is the ratio between these two values.

Temperature calibration is based on a run in which a temperature standard (indium) is heated through its melting transition. The recorded melting point of this standard (157.95 °C) is compared to the known melting point (156.60 °C), and the difference is calculated for temperature calibration. The same file used for the cell constant calibration can be used for this calibration.

All the experiments were carried out under a nitrogen atmosphere at about 5 °C to avoid any contamination that may due to chemical aging.

Before to perform the isothermal aging experiments, the samples were submitted to the following thermal history: The samples encapsulated in aluminium pans were heated in the DSC to a temperature approximately 30 °C above $T_g(T_0)$, during 10 min, in order to remove any thermal history of the samples. After the samples was quenched from T_0 to the aging temperatures (T_a), and then from this last temperature to $T_a/2$, and finally until the room temperature (T_r), approximately of 25 °C. Table 1 show to different cooling rates from T_0 to T_a (60, 70, 80, 90, 100 and 110 °C), from T_a to $T_a/2$, and finally from $T_a/2$ to temperature room. After thermal history have been erased, we use to different cooling rates for different aging temperatures. Several authors [4,15] did not indicate the cooling rate, other ones [6,16] used to the same coling rates for different aging temperatures. Based of the DSC experimental data, it can be observed that the new method applied is useful to reduce experimental scatter due to differences in cool transfer effects.

Then the samples, once removed to DSC, was annealing inside a glass tube in a thermostatic bath at different aging temperatures for aging times: 1, 2, 4, 6, 12, 24, 48, 72, 96, 120, 192, 240, 313 and 361 hours. After annealing, the samples was introduced into the DSC cell, quenched to starting temperature (25 °C) and inmediately heated until 250 °C at 10 °C/min. A second scan was made by quenching to temperature room and reheated at 10 °C/min in order to calculate the relaxation enthalpy. This scan will be used as reference scan.

3. Results and discussion

The glass transition temperature and the variation of the specific heat capacities (Δc_p) have been calculated using the method based on the intersection of both enthalpy–temperature lines for glassy and liquid states [6,17]. Glass transition temperature is taken as the midpoint of this transition. The calorimetric measurements (Δc_p and T_g)

Table 1
Different cooling rates from aging temperature (T_a) in the range 60–110 °C until the room temperature (T_r).

Cooling ramp

T_0=134ºC → T_r=25ºC

T_0 (°C)	Cooling rate (°C/min)	T_a (°C)	Cooling rate (°C/min)	$T_a/2$	Cooling rate (°C/min)	T_r (°C)
134	40	110	29	55	23	25
	38	100	28	50		
	36	90	27	45		
	34	80	26	40		
	32	70	25	35		
	30	60	24	30		

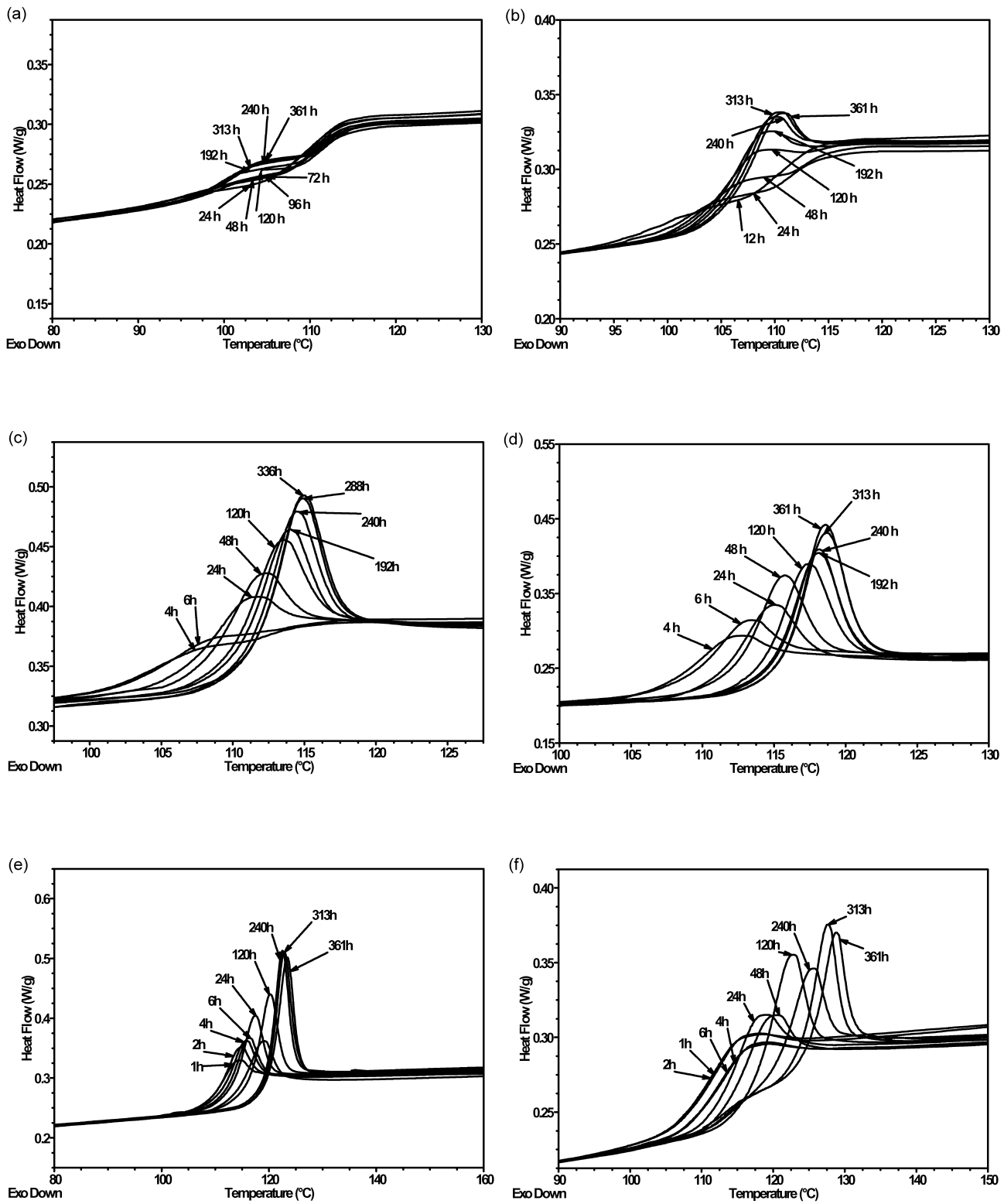

Fig. 1. (a) DSC scans of aged smple at 60 °C for different aging times. (b) DSC scans of aged sample at 70 °C for different aging times. (c) DSC scans of aged sample at 80 °C for different aging times. (d) DSC scans of aged sample at 90 °C for different aging times. (e) DSC scans of aged sample at 100 °C for different aging times. (f) DSC scans of aged sample at 110 °C for different aging times.

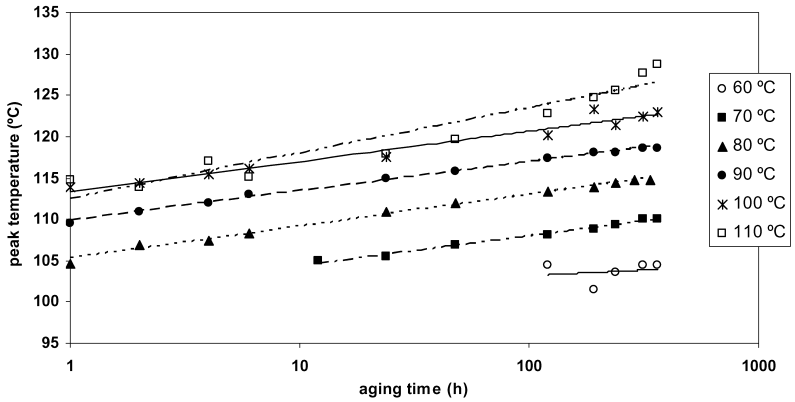

Fig. 2. Temperatures of endothermic peak (T_{ep}) versus logarithm of the aging time at different aging temperatures

were performed in quintuplicate. The average values obtained for these parameters are 0.31 ± 0.01 J/g °C and 104.8 ± 0.9 °C, respectively, in good agreement with other values published for similar systems [6,18–26].

The DSC thermograms of a sample with physical aging shows an endothermic peak whose position and intensity depends on aging conditions (temperature and time). This peak appear overhead on glass transition region. Fig. 1 shows DSC thermograms of aged system for different times at different temperatures: (a) 60 °C, (b) 70 °C, (c) 80 °C, (d) 90 °C, (e) 100 °C and (f) 110 °C. In these figures, at upper aging temperatures 80, 90, 100 and 110 °C, the temperature becomes high enough to afford mobility and then the network turn to the liquid equilibrium line producing the T_g-overshoot. At low aging temperatures the endothermic peak can be situated below T_g. Several authors have been reported this behaviour in epoxy resins [5–10]. The temperature of the endothermic peak increases in intensity with aging temperatures and displaces to higher temperatures with aging time.

Fig. 2 shows to the temperature of endothermic peak (T_{ep}) versus logarithm of the aging time at different aging temperatures. In this figure can be seen a linear increase of the T_{ep} with aging time in the range of 70–100 °C. The tendency of the T_{ep} seems deviate from linearity at 60 °C. This behaviour is not the same than was observed for other authors for amorphous polymers [3,6,10,27], where the deviation from linearity begins at 10 °C below T_g. Besides, this deviation can be observed at temperatures above T_g (110 °C).

Think of during the quenching to the temperature room (T_r) there is not process of relaxation and that the specific heat capacity (c_p) of the material is independent of aging time, and the relaxation enthalpy, Δh, can be calculated by the following expression:

$$\Delta h = \int_{T_r}^{T_0} (c_{p,aged} - c_{p,ref}) dT \quad (1)$$

where $c_{p,aged}$ and $c_{p,ref}$ are the specific heat capacities of sample aged and reference sample, respectively.

The Δh values calculate using Eq. (1) are plotted versus logarithm of aging time in Fig. 3, where it can be seen that the enthalpy relaxation increase with aging time. At temperatures below T_g, the relaxation enthalpy increase with temperature at the same aging times. The dependence of enthalpy relaxation seems to follow the relaxation of Bauwens–Crowet and Bauwens [16] at 100 °C. For aging temperature close to glass transition temperature, the relation predicts that each increase in aging time by a factor of ten causes an increase of relaxation enthalpy by 3 times Δc_p. Taking into account the following relation

$$\frac{d\Delta h}{d \ln t_a} = \frac{3\Delta c_p}{2.303} \quad (2)$$

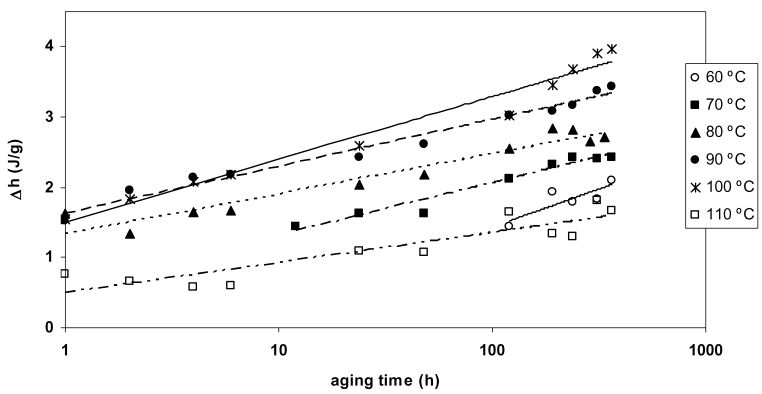

Fig. 3. Relaxation enthalpy versus logarithm of the aging time at different aging temperatures.

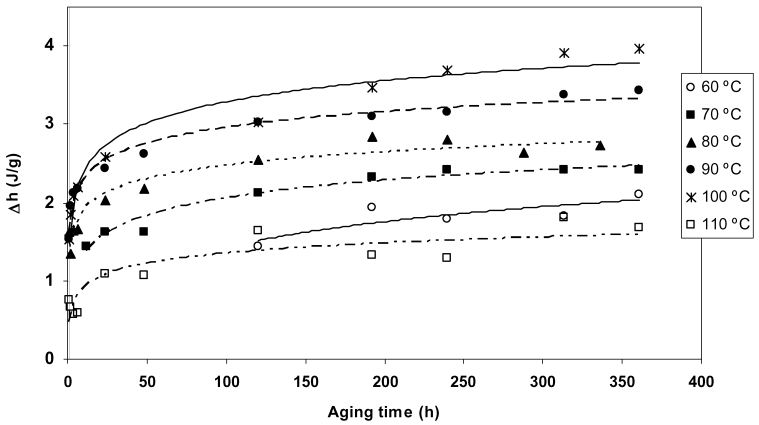

Fig. 4. Enthalpy relaxation versus aging time at different aging temperatures

The slope of the straight line (inflexional slope) of the plot of Δh versus aging time at 100 °C is about 2.85 times Δc_p, in good agreement with Bauwens–Crowet and Bauwens [16] and Montserrat [6]. Fig. 4 show the relaxation enthalpies versus aging time at aging temperatures in the range of 60–110 °C. These relaxation enthalpies increase until a aging time where becomes practically constant because of the structural equilibrium is achieved. In this figure can be seen that the relaxation enthalpy does not reach the equilibrium structural since the plots at different aging temperatures do not become constant for used aging times. The values of relaxation enthalpy at 110 °C are lower due to increase of the segmental mobility of chain segments of the epoxy network above T_g. The segmental mobility in thermosets may reflect the motions of chain segment and ends chain in crosslinked regions of network, and may also reflect the motions of segments of uncrosslinked molecules, which can be present in the full cured epoxy network.

It is very difficult to achieve experimentally a limiting enthalpy of relaxation (Δh_∞) for each aging temperature. Only can be calculated experimentally for values of aging temperature close to glass transition temperature [6]. This value cannot be determined experimentally in this study since increase even after the upper aging time. Though, there is several methods that let us to calculate (Δh_∞). The two methods selected for us, have been used previously by other authors [6,16,28] in the study of physical aging of epoxy resin. The first one of them is based in the extrapolation of the liquid enthalpy curve of the unaged sample:

$$\Delta h_\infty(T_a) = \int_{T_a}^{T_0} (c_{p,l} - c_{p,ref})dT \tag{3}$$

where T_a is aging temperature, $T_0 \approx 107$ °C, $c_{p,l}$ and $c_{p,ref}$ are the specific heat capacities of liquid state and reference sample, respectively.

The second one is a method that suppose the approximation of the previous method taking into account that (Δc_p) is independent of temperature:

$$\Delta h_\infty(T_a) = \Delta c_p(T_g - T_a) \tag{4}$$

where $T_g = 104.8$ °C, $\Delta c_p = 0.31$ J/g °C and T_a is the aging temperature.

Table 2 show the values of (Δh_∞) at different aging temperatures calculated by Eqs. (3) and (4). The values obtained for both methods present deviations that increase with annealing temperatures. The values calculate by Eqs. (3) and (4) are different to the estimated from Fig. 4, probably due to an overestimation of limiting relaxation enthalpy.

The fictive temperature (T_f) is a hypothetical temperature at which the structure of glass would be in equilibrium. According to Pérez et al. [28], and assuming that the fictive temperature of unaged sample is practically equal to glass transition temperature, the fictive temperature can be calculated using the following equation:

$$T_f \approx T_g - \frac{\Delta h}{\Delta c_p} \tag{5}$$

where T_g is the glass transition temperature, Δh is the relaxation enthalpy and Δc_p is the variation of the specific heat capacity. Fig. 5 shows fictive temperature versus aging temperature at different aging times. The fictive temperature decreases when the annealing time increases. Besides for a fixed aging time, the fictive temperature presents a minimum value. This minimum decreases with a aging

Table 2
Limiting relaxation enthalpy calculated using Eqs. (3) and (4) at different aging temperatures (T_a).

T_a (°C)	Δh_∞ (J/g) [Eq. (3)]	Δh_∞ (J/g) [Eq. (4)]
60	14.45	13.70
70	11.93	10.64
80	9.14	7.58
90	6.04	4.53
100	2.58	1.47
110	–	–

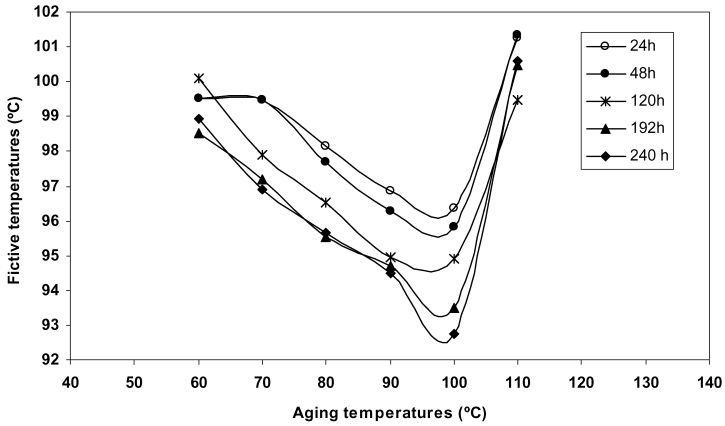

Fig. 5. Fictive temperatures versus aging temperature at different aging times.

time due to the glass is close to the structural equilibrium. This effect was observed for other authors in epoxy resins [3,6].

4. Conclusions

The study of physical aging of the epoxy network diglycidyl ether of bisphenol A (BADGE $n = 0$)/*m*-xylylenediamine shows the endothermic aging peak and relaxation enthalpy that increase gradually with aging time at aging temperatures close to T_g. For a fixed time, the relaxation enthalpy increase with temperature at temperatures below T_g. At temperatures above T_g, as 110 °C, the values of enthalpy are lesser than those obtained at 60 °C due to increase of motions of the chains in the epoxy network.

The fictive temperature decreases until a minimum where the glass is close to structural equilibrium. This parameter is basic in order to describe the effect of physical aging at annealing temperatures near to T_g.

References

[1] Chartoff RP. Thermoplastics polymers. In: Turi EA, editor. Thermal characterization of polymeric materials. San Diego: Academic Press; 1997.
[2] Prime RB. In: Turi EA, editor. Thermal characterization of polymeric materials. San Diego: Academic Press; 1981.
[3] Plazek DJ, Frund ZN. J Polym Sci Polym Phys 1990;28:431.
[4] Lee A, McKenna GB. Polymer 1988;29:1812.
[5] Barral L, Cano J, López J, López-Bueno I, Nogueira P, Abad MJ, Ramirez C. J Therm Anal Calorim 2000;60:391.
[6] Montserrat S. J Polym Sci Polym Phys 1994;32:509.
[7] G'Sell C, McKenna GB. Polymer 1992;33:2103.
[8] Lee A, McKenna GB. Polymer 1990;31:423.
[9] Montserrat S. J Therm Anal Calorim 1993;40:553.
[10] Jong SR, Yu TL. J Polym Sci Polym Phys 1997;35:69.
[11] Cortes P, Montserrat S. J Non-Cryst Solids 1994;172–174:622.
[12] McKenna GB. In: Booth CP, editor. Polymer properties. Comprehensive polymer science, vol. 2. Oxford: Pergamon; 1989.
[13] Lee H, Neville K. Handbook of epoxy resin. New York: McGraw-Hill; 1967.
[14] May CA. Epoxy resins: chemistry and technology. New York: Marcel Dekker; 1988.
[15] Cowie JMG, Ferguson R. Macromolecules 1989;22:2312.
[16] Bauwens-Crowet C, Bauwens JC. Polymer 1986;27:709.
[17] Richardson MJ, Savil NG. Polymer 1975;16:735.
[18] Fraga F, Salgado T, Rodríguez Añón JA, Núñez L. J Therm Anal 1994;41:1543.
[19] Núñez L, Fraga F, Salgado T, Rodríguez Añón JA. Pure Appl Chem 1995;67:1091.
[20] Núñez L, Fraga F, Fraga L, Castro A. J Appl Polym Sci 1997;63:635.
[21] Núñez L, Taboada J, Fraga F, Núñez MR. J Appl Polym Sci 1997;66:1377.
[22] Núñez L, Fraga F, Castro A, Núñez MR. Villanueva. J Appl Polym Sci 1998;70:1931.
[23] Núñez L, Fraga F, Castro A, Núñez MR, Villanueva M. J Appl Polym Sci 2000;75:291.
[24] Núñez L, Fraga F, Castro A, Núñez MR, Villanueva M. Polymer 2001;42:3581.
[25] Riccardi CC, Fraga F, Dupuy J, Williams RJJ. J Appl Polym Sci 2001;82:2319.
[26] Fraga F, Burgo S, Rodríguez-Núñez E. J Appl Polym Sci 2001;82:3366.
[27] ten Brinke G, Grooten R. Colloid Polym Sci 1989;267:992.
[28] Perez J, Cavaille JY, Diaz-Calleja R, Gómez-Ribelles JL, Monleón-Pradas M, Ribes Graus A. Makromol Chem 1991;192:2141.